

# Synthesis and Characterization Barium M-Hexaferrites ( $\text{BaFe}_{12-2x}\text{Co}_x\text{Mn}_x\text{Ni}_x\text{O}_{19}$ ) as a Microwave Absorbent Material

*by Susilawati Susilawati*

---

**Submission date:** 09-Jun-2021 04:24PM (UTC+0700)

**Submission ID:** 1603363259

**File name:** susilawati\_dan\_aris\_doyan\_SSP.317.46.pdf (1.89M)

**Word count:** 2862

**Character count:** 14626

## Synthesis and Characterization Barium M-Hexaferrites ( $\text{BaFe}_{12-2x}\text{Co}_x\text{Mn}_x\text{Ni}_x\text{O}_{19}$ ) as a Microwave Absorbent Material

SUSILAWATI Hambali<sup>1,a,\*</sup> and ARIS Doyan<sup>2,b</sup>

<sup>1,2</sup>Master of Science Education Program, University of Mataram, Lombok, West Nusa Tenggara, Indonesia.

<sup>a</sup>susilawatihambali@unram.ac.id, <sup>b</sup>aris\_doyan@unram.ac.id

**Keywords:** Synthesis, Characterization, Absorbent Material, Barium M-hexaferrite, Microwave.

**Abstract.** This study aims to synthesize microwave absorbent material from barium M-Hexaferrite doped Co-Mn-Ni ions ( $\text{BaFe}_{12-2x}\text{Co}_x\text{Mn}_x\text{Ni}_x\text{O}_{19}$ ) using co-precipitation method with varying concentrations ( $x = 0.2, 0.4, 0.6, 0.8,$  and  $1.0$ ) and calcinations temperatures in the range of  $200$  to  $800^\circ\text{C}$ . The samples characterization was conducted to investigate the effect of doping concentration variations on the electrical, magnetic and microwave absorption properties using X-Ray Diffraction (XRD), Scanning Electron Microscope (SEM-EDX), Transmission Electron Microscope (TEM), Vibrating Sample Magnetometer (VSM), and Network Vector Analyzer (VNA). The results from XRD characterization showed that the sample formed the barium iron oxide ( $\text{BaFe}_{12}\text{O}_{19}$ ) phase with  $a = b = 5.03\text{\AA}$  and  $c = 13.43\text{\AA}$ . The results of SEM-EDX and TEM samples of  $\text{BaFe}_{9.6}\text{Co}_{0.8}\text{Mn}_{0.8}\text{Ni}_{0.8}\text{O}_{19}$  showed that the sample size ranged from  $79$ - $165$  nm in the hexagonal crystal structure form. The magnetic properties with VSM indicate that the sample coercivity value decreases significantly from  $0.41$  T at  $x = 0.0$  to  $0.09$  T at  $x = 0.8$ , indicating that the sample is soft magnetic. The value of electrical conductivity is in the range of  $2.42 \times 10^{-4}$  to  $9.30 \times 10^{-4}$  S/cm shows that the sample is a semiconductor. Analysis of the absorption properties of microwaves with VNA produced maximum permittivity and permeability values of  $28.40$  and  $54.40$  at  $10.30$  GHz, and a maximum Reflection Loss (RL) value of  $-20.20$  dB at a frequency of  $15$  GHz with an absorption coefficient of  $99.05$  % at concentration  $x = 0.6$ . The high permittivity, permeability, RL, and absorption coefficients indicate that the  $\text{BaFe}_{12-2x}\text{Co}_x\text{Mn}_x\text{Ni}_x\text{O}_{19}$  sample has the potential to be a microwave absorbent material on X-band to Ku-band frequency.

### Introduction

The increasing electromagnetic interference pollution in the environment is the impact of technological developments, so it is necessary to research microwave absorber material. Barium M-Hexaferrite ( $\text{BaFe}_{12}\text{O}_{19}$ ) is a permanent magnetic material that has high chemical stability and is resistant to corrosion and can be applied as a microwave absorber [1]. The characteristics of Barium M-Hexaferrite (BaM) are a hexagonal molecular structure, high Curie temperature ( $450^\circ\text{C}$ ), and a large coercivity field ( $6700$  Oe), the saturation magnetization of  $78$  emu/g, good corrosion resistance and chemical stability, can regulate electrical properties and magnets according to application requirements. BaM is less effective to be used as a microwave absorber material because of the large coercivity field so that the absorption rate is small. This problem can be overcome by adding doping or substituting  $\text{Fe}^{3+}$  ions with  $\text{Al}^{3+}$ ,  $\text{Ga}^{3+}$ , and  $\text{Cr}^{3+}$  [2] to reduce the magnetic properties of BaM from hard magnetic to soft magnetic.

Several studies have been carried out to change the characteristics of BaM by adding ions. As for the ions that have been used such as Mn-Ni, Co-Mn, Co-Zn [3,4]. This study uses a combination of three Co-Mn-Ni ions because it has the same configuration as the  $\text{Fe}^{3+}$  ion [5,6]. The results of the study analyzed the magnetic and electrical properties of the resulting barium M-Hexaferrite doped Co-Mn-Ni ions can be applied as a microwave absorber material.

## Experimental

The synthesis samples were synthesized material  $\text{FeCl}_3$  and  $\text{BaCO}_3$ . Both materials were dissolved using distilled water,  $\text{HCl}$  (hydrochloric acid), and  $\text{NH}_4\text{OH}$ . The ingredients for doping are  $\text{NiCl}_2 \cdot 6\text{H}_2\text{O}$  (Nickel (II) Chloride Hexahydrate) and  $\text{CoCl}_2 \cdot 6\text{H}_2\text{O}$  (Cobalt (II) Chloride Hexahydrate) and  $\text{MnCl}_2$  [7, 8]. The characterization was carried out using X-Ray Diffractometer (XRD), Scanning Electron Microscopy (SEM-EDX), Transmission Electron Microscope (TEM), Vibrating Sample Magnetometer (VSM) and Vector Network Analyzer (VNA) to identify phases, the distribution of elements particle size. Knowing the distribution and the percentage of each element direct information on the magnetic and electrical properties will be obtained [9].

## Result and Discussion

Fig. 1 (a, b) shows that there are a shift of angle  $2\theta$  and an increase in peak intensity with increasing doping concentration. The angular displacement  $2\theta$  indicates the replacement of  $\text{Fe}^{3+}$  ions by doping ions, and this process causes lattice expansion which is indicated by changes in lattice constant values (Table 1). The increase in doping concentration causes an increase in the value of the lattice constant [10,11]. Then with the change in concentration causes an increase in the peak intensity and size of the crystal. The lattice constant data obtained at ( $x = 0.8$ ) are  $a = b = 5.89 \text{ \AA}$ ,  $c = 13.94 \text{ \AA}$ , and the ratio of  $c/a = 2.36$ . The data from the comparison of  $c/a$  shows less than 3.98 which means that there was a formation of hexagonal structure [12].

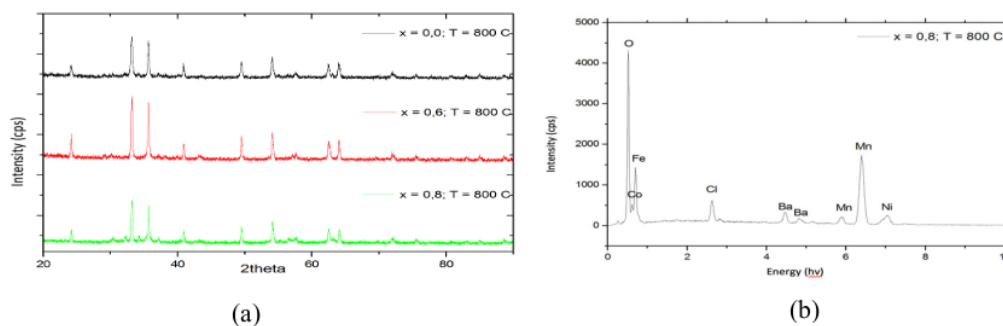


Fig. 1: (a,b) XRD analysis of  $\text{BaFe}_{12-2x}\text{Co}_x\text{Mn}_x\text{Ni}_x\text{O}_{19}$  samples

Table 1: Analysis XRD samples of  $\text{BaFe}_{12-2x}\text{Co}_x\text{Ni}_x\text{O}_{19}$

| Samples   | $a = b$<br>( $\text{\AA}$ ) | $c$ ( $\text{\AA}$ ) | $c/a$ | $V$ ( $\text{\AA}^3$ ) | $D$<br>(nm) |
|-----------|-----------------------------|----------------------|-------|------------------------|-------------|
| $x = 0.0$ | 5.03                        | 13.43                | 2.67  | 339.73                 | 29.60       |
| $x = 0.6$ | 5.76                        | 13.71                | 2.38  | 454.83                 | 37.60       |
| $x = 0.8$ | 5.89                        | 13.94                | 2.36  | 472.04                 | 40.20       |

The results of SEM-EDX characterization based on Fig. 2a shows that the particle size is in nano order range, from 41 nm to 151 nm with even distribution of each element in the  $\text{BaFe}_{10}\text{Co-NiO}_{19}$  sample (Fe = 58.84%; O = 18.14%; Ba = 9.45%; Co = 4.81%; Ni = 1.07%, and a few impurities, Cl = 3.04%) (Table 2). The characterization with TEM (Fig. 2b) shows the sample has a hexagonal structure, but the resulting hexagonal structure has not been formed completely because the resulting phase is not a single phase [13].

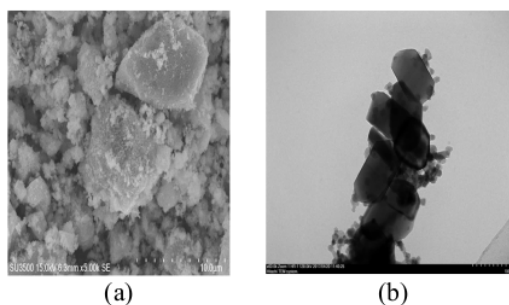


Fig. 2: Characterization of a) SEM and b) TEM for  $\text{BaFe}_{12-2x}\text{Co}_x\text{Mn}_x\text{Ni}_x\text{O}_{19}$  sample

Table 2: Elements in the  $\text{BaFe}_{10}\text{Co-NiO}_{19}$  sample

| Elements | Weight (%) | Atomic (%) | Error (%) |
|----------|------------|------------|-----------|
| O        | 18.14      | 44.87      | 6.31      |
| Cl       | 3.04       | 3.4        | 6.49      |
| Ba       | 9.45       | 2.72       | 11.53     |
| Mn       | 4.65       | 3.35       | 9.69      |
| Fe       | 58.84      | 41.71      | 3.31      |
| Co       | 4.81       | 3.23       | 12.77     |
| Ni       | 1.07       | 0.72       | 44.8      |

The magnetism of the sample is shown in Table 3 and Figs. 3 (a - c). BaM which was synthesized with  $\text{FeCl}_3$  as a raw material has an  $H_c$  value of 6.7 T and  $M_s$  value of 72 emu/ gram. The results showed the value of  $H_c$  for  $x = 0.0$ ; 0.6; and 0.8 the magnitude of each is 0.41, 0.10, and 0.09 T. This means that the value of  $H_c$  has decreased along with the increasing number of Co-Mn-Ni doping, while the value of  $M_s$  and  $M_r$  has increased. The increase in  $M_s$  and  $M_r$  values is caused by the decrease in the anisotropic crystalline magneto resulting in a decreased  $H_c$  value. The decrease in  $H_c$  value causes the sample hysteresis curve to narrow as shown in Fig. 3 (a - c). The decrease in  $H_c$  value indicates that the magnetic properties of the sample have been successfully reduced from hard magnetic to soft magnetic so that the  $\text{BaFe}_{12-x}\text{Co}_x\text{Mn}_x\text{Ni}_x\text{O}_{19}$  sample with natural iron sand base material doped with Co-Mn-Ni ions, can be used as a microwave absorber material because the radar absorbing mineral is best at a low coercivity value of 0.11 T at  $x = 0.4$  [14].

Table 3: Magnetism properties of  $\text{BaFe}_{12}\text{O}_{19}$  samples at different dopings

| $x$ | Samples  | $M_r$ (emu/g) | $M_s$ (emu/g) | $H_c$ (T) |
|-----|--|---------------|---------------|-----------|
| 0.0 | $\text{BaFe}_{12}\text{O}_{19}$                          | 2.79          | 4.37          | 0.41      |
| 0.6 | $\text{BaFe}_{10.8}(\text{Co-Mn-Ni})_{0.6}\text{O}_{19}$ | 4.75          | 11.70         | 0.10      |
| 0.8 | $\text{BaFe}_{10}(\text{Co-Mn-Ni})_{1.0}\text{O}_{19}$   | 6.26          | 15.30         | 0.09      |

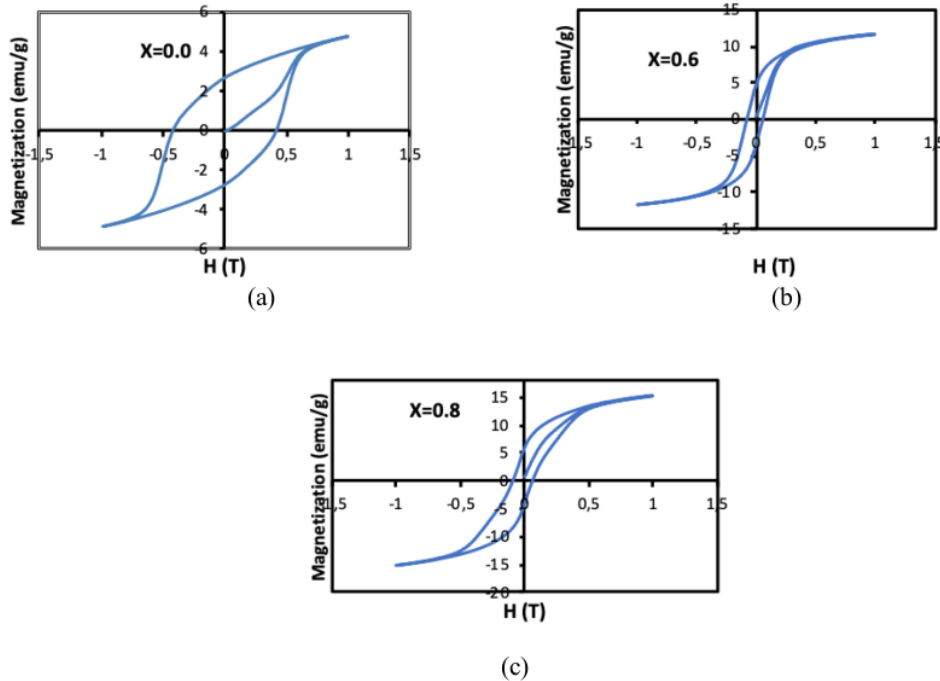


Fig. 3: Sample hysteresis curves of a)  $\text{BaFe}_{12}\text{O}_{19}$ , b)  $\text{BaFe}_{10.8}(\text{Co-Mn-Ni})_{0.6}\text{O}_{19}$ , c)  $\text{BaFe}_{10}(\text{Co-Mn-Ni})_{1.0}\text{O}_{19}$

The electrical nature of the sample (conductivity value) is known through the VNA test. The conductivity values of the samples are in the range of  $7.24 \times 10^{-4}$  -  $3.53 \times 10^{-4}$  S/cm for samples  $x = 0.0$ ,  $9.31 \times 10^{-4}$  -  $2.42 \times 10^{-4}$  S/cm for samples  $x = 0.6$  and  $6.25 \times 10^{-4}$  -  $2.83 \times 10^{-4}$  S/cm for samples  $x = 0.8$ . The resulting conductivity value indicates that the sample is in the range of semiconductor properties of  $10^{-7}$ - $10^3$  S/cm [15]. The requirement for a mineral to be used as a microwave absorbing mineral is that the material must possess the ability to convert energy [16].

The permeability,  $\mu$  and permittivity,  $\epsilon$  values of samples in complex numbers are shown in Fig. 4 (a - d), the magnitude of the microwave energy stored in the material is indicated by the real value, while the magnitude of the dissipated microwave energy in the form of energy loss is shown by the imaginary value [17]. The working frequency area of the microwave absorbing material is determined by a combination of real and imaginary values. The value of  $\epsilon'$  (real permittivity) for all three samples tends to remain at the frequency of 10.00 to 10.23 GHz, while starting to increase at the frequency of 10.25 to 15.00 GHz. The increase in  $\epsilon'$  is caused by an increase in doping value and heating temperature (from 1.98 to 28.40). Increasing the value of  $\epsilon'$  as a result of the transformation of  $\text{Fe}^{3+}$  ions to  $\text{Fe}^{2+}$  ions causing polarization on the surface of the sample [18].

It is clearly shown in Fig. 4(a) and (b) that real permeability value is greater than that of imaginary which means that the ability of the sample to release electrical energy is smaller than forming an electric field [19]. Graphs in Figs. 4(c) and (d) show the relationship between frequency and permeability. The permeability value decreases with the increasing number of moles of doping material and calcination temperature. Besides, the real permeability value ( $\mu'$ ) produced is higher than the imaginary permeability ( $\mu''$ ).

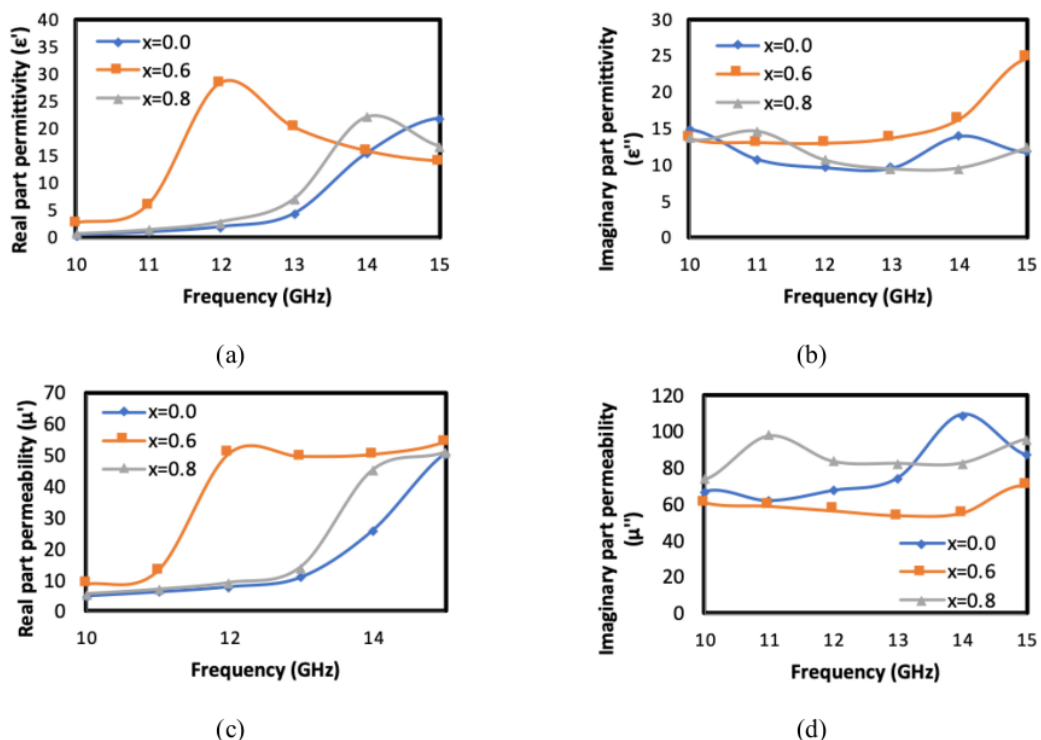


Fig. 4: Permittivity and permeability values of  $\text{BaFe}_{12-2x}\text{Co}_x\text{Mn}_x\text{Ni}_x\text{O}_{19}$  samples

Fig. 5(a) depicted the relationship between the dielectric loss tangent ( $\delta e$ ) and frequency. The figure shows that the resulting value  $\delta e$  decreases (near zero) at the frequency (13-15) GHz. These results reinforce that the ability of the sample to release electrical energy is smaller than forming an electric field. Fig. 5(b) shows the relationship between magnetic loss tangent ( $\delta m$ ) and frequency where the value of  $\delta m$  decreases with an increasing number of moles of doping material where the decreasing value of  $\delta m$  is caused by a decrease in interfacial polarization as a result of support [20].

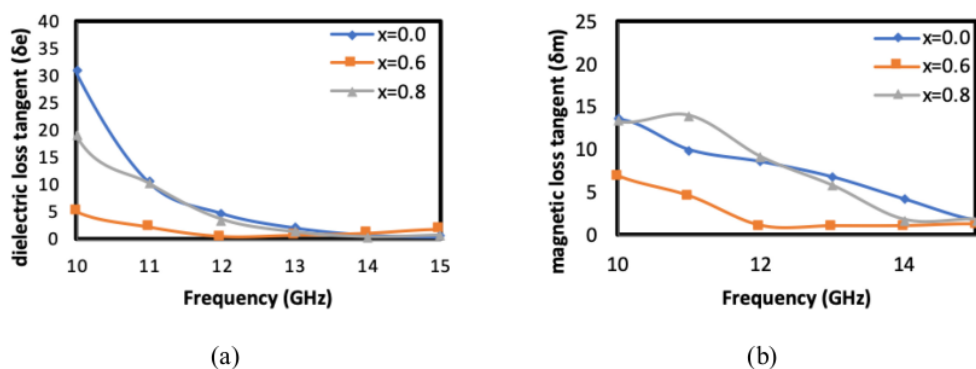


Fig. 5: Graph of the relationship between a) tangent dielectric loss and b) magnetic loss tangent of  $\text{BaFe}_{10}\text{Co-Mn-NiO}_{19}$  samples in the frequency range (10-15) GHz

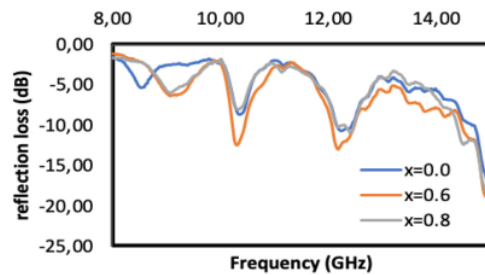


Fig. 6: Graph of reflection loss samples

The value of absorption intensity or Reflection Loss (RL) is shown in Fig. 6. At a frequency of 15 GHz in the  $\text{BaFe}_{10}\text{Co-Mn-NiO}_{19}$  sample, RL has a maximum value of -20.20 dB and absorbs coefficient of 99.05% for the concentration  $x = 0.6$ . This shows that the higher Co-Mn-Ni doping concentration and heating temperature causes the absorption coefficient and RL value to be generated even higher. This means that the ability to absorption of microwaves is greater [21].

### Conclusions

The crystal structure of  $\text{BaFe}_{12-2x}\text{Co}_x\text{Mn}_x\text{Ni}_x\text{O}_{19}$  sample of natural iron sand is hexagonal with particle size in nano order. The conductivity value of the sample is in the range of semiconductor. The magnetism of the sample indicates that it has succeeded in reducing from hard magnetic to soft magnetic, because the coercivity value of the sample has decreased. As for the 15 GHz frequency of the  $\text{BaFe}_{12-2x}\text{Co}_x\text{Mn}_x\text{Ni}_x\text{O}_{19}$  sample, RL has a maximum value of -20.20 dB and absorbs coefficient of 99.05%. These results indicate that the  $\text{BaFe}_{12-2x}\text{Co}_x\text{Mn}_x\text{Ni}_x\text{O}_{19}$  sample can be applied as a material that can absorb microwaves.

### References

- [1] I. N. Saidah, M. Zainuri, Effect of pH Variation on HCl Solvents in the Synthesis of Barium M-Hexaferrit with Zn Doping ( $\text{BaFe}_{11}, 4\text{ZnO}, 6\text{O}_{19}$ ) Using the Coprecipity Method, *Jurnal Sains dan Seni ITS* 1(1) (2012) B41-B46. DOI: 10.12962/j23373520.v1i1.354.
- [2] D. A. Vinnik, D. A. Zhrebtsov, L. S. Mashkovtseva, S. Nemrava, M. Bischoff, N. S. Perov, R. Niewa, Growth, structural and magnetic characterization of Al-substituted barium hexaferrite single crystals, *J. of Alloys and Compounds* 615 (2014) 1043-1046. DOI: 10.1016/j.jallcom.2014.07.126.
- [3] Susilawati, A. Doyan, Sahlam, Synthesis and Characterization Materials M-Barium Hexaferrite Doping Ions Co-Mn NanoParticle, In *IOP Conference Series: Materials Science and Engineering* 196(1) (2017) 012016. IOP Publishing. DOI: 10.1088/1757-899X/196/1/012016.
- [4] Susilawati, A. Doyan, M. Munib, Synthesis by co-precipitation method and characterization of Nickel-doped Barium M-Hexaferrite ( $\text{BaFe}_{12}\text{O}_{19}$ ), *Proceeding ICMSE* (2015). ISBN 9786021570425.
- [5] H. Sözeri, H. Deligöz, H. Kavas, A. Baykal, Magnetic, dielectric and microwave properties of M-Ti substituted barium hexaferrites (M=  $\text{Mn}^{2+}$ ,  $\text{Co}^{2+}$ ,  $\text{Cu}^{2+}$ ,  $\text{Ni}^{2+}$ ,  $\text{Zn}^{2+}$ ), *Ceramics International* 40(6) (2014) 8645-8657. DOI: 10.1016/j.ceramint.2014.01.082.
- [6] R. Agustianto, W. Widyastuti, Mol Fraction and Ph Variation of Magnetic Properties and Micro Structure of Barium Hexaferrit Using the Sol-Gel Auto Combustion Method, *Journal of Engineering ITS* 3(1) (2014) F108-F112.

- 
- [7] J. Li, H. Zhang, V. G. Harris, Y. Liao, Y. Liu, Ni–Ti equiatomic co-substitution of hexagonal M-type  $\text{Ba}(\text{NiTi})_x\text{Fe}_{12-2x}\text{O}_{19}$  ferrites, *Journal of Alloys and Compounds* 649 (2015) 782-787. DOI: 10.1016/j.jallcom.2015.07.173.
- [8] F.R. Sholihah, M. Zainuri, Effect of Holding Time Calcination on the Magnetic Properties of Barium M-Hexaferrite ( $\text{BaFe}_{12-x}\text{Zn}_x\text{O}_{19}$ ) with Zn Doping Ion, *Journal of Science and Art ITS* 1(1) (2012) B25-B29.
- [9] Susilawati, A. Doyan, M. Taufik, Wahyudi, E. R. Gunawan, A. Fitriani, Nazarudin, Characterization of Barium M-Hexaferrite with Doping Zn and Mn for Microwaves Absorbent, *Journal Materials Science Forum* 966 (2019) 283-289. DOI: 10.4028/www.scientific.net/MSF.966.282.
- [10] T.R. Wagner, Preparation and crystal structure analysis of magneto plumbite type  $\text{BaGa}_{12}\text{O}_{19}$ , *J. Solid State Chem.* 136 (1998) 120–124. DOI: 10.1006/jssc.1997.7681.
- [11] Susilawati, A. Doyan, M. Munib, Synthesis by Co-precipitation Method and Characterization of Nickel-doped Barium M-Hexaferrite ( $\text{BaFe}_{12}\text{O}_{19}$ ), *Proceeding ICMSE* (2015). ISBN 9786021570425.
- [12] L.N. Usvanda, M. Zainuri, Synthesis, and Characterization of BaM/PANi Radar Absorbing Material (RAM) Layer Based on X-Band Wave Range with Thickness Variation, *Journal of Science and Art ITS* 5(2) (2016). DOI: 10.12962/j23373520.v5i2.17900.
- [13] D.T. Rahmawati, D.H. Kusumawati, M. Si, L. Rohmawati, Variation of  $\text{Fe}_3\text{O}_4$  Addition to Pani /  $\text{Fe}_3\text{O}_4$  Alloys for Microwaves, *Journal of Physics* 4 (1) (2015) 1-5.
- [14] L.M. Said, Analysis of the Properties of Electrical Conductivity in Several Types of Materials with the Remote Potential Method, *Jurnal Teknosains* 7 (2013) 66-67. DOI: 10.24252/teknosains.v7i1.74.
- [15] S. H. Mahmood, A. N. Aloqaily, Y. Maswadeh, A. Awadallah, I. Bsoul, M. Awawdeh, H. Juwhari, Effects of Heat Treatment on the Phase Evolution, Structural, and Magnetic Properties of Mo-Zn Doped M-type Hexaferrites, *Solid State Phenomena* 232 (2015) 65-92. DOI: 10.4028/www.scientific.net/SSP.232.65.
- [16] H. Sözeri, H. Deligöz, H. Kavas, A. Baykal: Magnetic, dielectric and microwave properties of M–Ti substituted barium hexaferrite (M=  $\text{Mn}^{2+}$ ,  $\text{Co}^{2+}$ ,  $\text{Cu}^{2+}$ ,  $\text{Ni}^{2+}$ ,  $\text{Zn}^{2+}$ ), *Ceramics International* 40(6) (2014) 8645-8657. DOI: 10.1016/j.ceramint.2014.01.082.
- [17] C. J. Li, B. Wang, J.N. Wang, Magnetic and microwave absorbing properties of electrospun  $\text{Ba}_{(1-x)}\text{La}_x\text{Fe}_{12}\text{O}_{19}$  nanofibers, *Journal of Magnetism and Magnetic Materials* 324(7) (2012) 1305-1311. DOI: 10.1016/j.jmmm.2011.11.016.
- [18] W. Zhang, Y. Bai, X. Han, L. Wang, X. Lu, L. Qiao, Magnetic properties of Co–Ti substituted barium hexaferrite, *Journal of Alloys and Compounds* 546 (2013) 234-238.
- [19] Susilawati, A. Doyan, Khaililurrahman, Synthesis and Characterization of Barium Hexaferrite with Manganese (Mn) Doping Material as Anti-Radar, *American Institute of Physics Conf. Proc.* 1801 (2016) 040007. DOI: 10.1063/1.4973096.
- [20] V.N. Dhage, M.L. Mane, M.K. Babrekar, C.M. Kale, K.M. Jadhav, Influence of chromium substitution on structural and magnetic properties of  $\text{BaFe}_{12}\text{O}_{19}$  powder prepared by sol-gel auto combustion method, *Journal of Alloys and Compounds* 509(12) (2011) 4394-4398. DOI: 10.1016/j.jallcom.2011.01.040.
- [21] R.S. Alam, M. Moradi, M. Rostami, H. Nikmanesh, R. Moayedi, Y. Bai, Structural, magnetic and microwave absorption properties of doped Barium-hexaferrite nano-particles synthesized by the co-precipitation method, *Journal of Magnetism and Magnetic Materials* 381(2015) 1-9. DOI: 10.1016/j.jmmm.2014.12.059.



# Synthesis and Characterization Barium M-Hexaferrites (BaFe<sub>12-2x</sub>CoxMnxNixO<sub>19</sub>) as a Microwave Absorbent Material

## ORIGINALITY REPORT

6%

SIMILARITY INDEX

%

INTERNET SOURCES

%

PUBLICATIONS

6%

STUDENT PAPERS

## PRIMARY SOURCES

1

Submitted to Universiti Sains Islam Malaysia

Student Paper

3%

2

Submitted to Universitas Mataram

Student Paper

2%

3

Submitted to Coventry University

Student Paper

1%

4

Submitted to Universiti Putra Malaysia

Student Paper

<1%

Exclude quotes On

Exclude matches < 1 words

Exclude bibliography On